Inorg. Chem. **2007**, 46, 8170–8181

Inorganic Chemistry Article

Chiral Recognition and Conglomerate Crystallization Induced by Self-Organization of Cobalt(III) Complexes of a Tripodal Ligand Containing Three Imidazole Groups

Hirofumi Nakamura,[†] Yukinari Sunatsuki,[†] Masaaki Kojima,*[,†] and Naohide Matsumoto[‡]

Department of Chemistry, Faculty of Science, Okayama University, Tsushima-naka 3-1-1,
Okayama 700-8530, Japan, and Department of Chemistry, Faculty of Science,
Kumamoto University, Kurokami 2-39-1, Kumamoto 860-8555, Japan

Received February 13, 2007

The effect of a counteranion on chiral recognition inducing conglomerate crystallization of a cobalt(III) complex is reported. An achiral tripodal ligand involving three imidazole groups, tris{[2-{(imidazol-4-yl)methylidene}amino]-ethyl}amine (H_3L), was prepared by condensation of tris(2-aminoethyl)amine and 4-formylimidazole in a 1:3 mole ratio. The reaction of H_3L and *trans*-$[Co^{III}Cl_2(py)_4]^+$ afforded the chiral (Δ or Λ) $[Co^{III}(H_3L)]^{3+}$ complex. The formally hemideprotonated complexes $[Co^{III}(H_{1.5}L)]X_{1.5}\cdot nH_2O$ (where X = Cl, Br, I, BF_4, ClO_4, or PF_6) were synthesized by controlled deprotonation of the uncoordinated imidazole NH groups of $[Co(H_3L)]^{3+}$. In crystals of the hemideprotonated complex, two components, $[Co(H_3L)]^{3+}$ and [Co(L)], with the same absolute configuration are linked by imidazole–imidazolate hydrogen bonds to form an extended homochiral 2D sheet structure, which is composed of a hexanuclear unit with a trigonal void. There are two ways of stacking the sheets: One is via homochiral stacking, and the other is via heterochiral stacking. When the size of the counterion is small (i.e., X = Cl, Br, I, or BF_4), adjacent homochiral sheets with the same chirality are stacked to form a homochiral crystal (conglomerate). With large anions (i.e., ClO_4^- and PF_6^-), a homochiral sheet consisting of Δ enantiomers and a sheet consisting of Λ enantiomers are stacked alternately to give a heterochiral crystal (a racemic crystal). Optically active Λ-$[Co(H_{1.5}L)](ClO_4)_{1.5}\cdot H_2O$ was synthesized from Λ-$[Co(H_3L)]^{3+}$, and the crystal structure was compared to that of the racemic complex. There are two conflicting factors governing the crystal structure: the skeletal density; the size of the channels. The 2D sheets are more closely packed in the homochiral crystal than in the heterochiral crystal. However, the channels, where the counterions are accommodated, are smaller in the homochiral crystal, and the steric congestion between the anions increases with increasing anion size. The heterochiral crystal has a flexible, zigzag channel structure, and the size of the channels can increase to accommodate larger anions. Thus, complexes with large anions (i.e., ClO_4^- and PF_6^-) preferentially form heterochiral crystals rather than homochiral crystals.

Introduction

The most beautiful experiment in the history of chemistry, according to a survey of *Chem. Eng. News* readers, is Louis Pasteur's manual separation of sodium ammonium tartrate crystals into two sets of crystals that were mirror images of each other.[1a] The experiment was the effective beginning of stereochemistry and understanding molecules in three dimensions.[1,2] When a racemate aggregates and condenses, it can form the following: (1) a racemic crystal (it is also called a racemic compound or a true racemate in which the two enantiomers are present in equal quantities in a well-defined arrangement within the crystal lattice); (2) a conglomerate (a mechanical mixture of crystals of the pure enantiomers); (3) a racemic solid solution (a pseudoracemate).[3] A conglomerate is formed as a result of a spontaneous resolution. Although spontaneous resolution is most often observed in crystals, it is also observed in other media, such as liquid

---

* To whom correspondence should be addressed. E-mail: kojima@cc.okayama-u.ac.jp. Fax: +81-86-251-7842.

[†] Okayama University.

[‡] Kumamoto University.

(1) (a) Freemantle, M. *Chem. Eng. News* **2003**, *81* (34), 27−30. (b) Pasteur, L. *Ann. Chim. Phys.* **1848**, *24*, 442−459. (c) Kauffman, G. B.; Bernal, I.; Schütt, H.-W. *Enantiomer* **1999**, *4*, 33−45.

(2) (a) Perez-Garcia, L.; Amabilino, D. B. *Chem. Soc. Rev.* **2004**, *31*, 342−356. (b) Eliel, E. L.; Wilen, S. H. *Stereochemistry of organic Compounds*; Wiley: New York, 1994.

10.1021/ic070286+ CCC: $37.00

crystals and self-assembled monolayers.[4] The separation of two enantiomers forming a conglomerate does not require any optically active auxiliary agent, and thus, this is the most straightforward route to the pure enantiomers.[3b] Most racemates (>90%) crystallize as racemic crystals; the formation of a conglomerate is rare and is not predictable,[3a] and thus, the creation of a compound forming a conglomerate is difficult. However, if there are preferential and extended homochiral interactions between neighboring chiral units, the chirality can be extended to higher dimensionality, and hence, conglomerate crystallization is likely to occur.[5] These chiral discriminative interactions may arise from coordination bonds and/or hydrogen bonds, which are substantially strong, selective, and directional. In a previous paper,[6] we reported on a molecular system inducing conglomerate crystallization, where a chiral molecule generated from achiral components gives a homochiral two-dimensional (2D) sheet via self-organization and intermolecular homochiral interaction and sheets with the same chirality are stacked in the crystal to form a conglomerate. Figure 1 shows a schematic representation of the procedure. We have designed a cobalt(III) complex with an achiral tripodal ligand involving three imidazole groups, tris{[2-{(imidazol-4-yl)methylidene}-amino]ethyl}amine (H_3L, Figure 1a). The $[Co^{III}(H_3L)]^{3+}$ complex is chiral with either a Δ (clockwise) or a Λ (anticlockwise) configuration, due to the screw coordination arrangement of the achiral tripodal ligand around the Co^{III} ion (Figure 1b). The uncoordinated imidazole NH groups can be easily deprotonated by the action of a base.[7] The formally hemideprotonated species, $[Co^{III}(H_{1.5}L)]Cl_{1.5}\cdot 4H_2O$ (i.e., $[Co^{III}(H_3L)][Co^{III}(L)]Cl_3\cdot 8H_2O$, **2Cl**), was prepared by controlled deprotonation of $[Co^{III}(H_3L)]Cl_3$ (**1Cl**). In a crystal of **2Cl**, two components, $[Co(H_3L)]^{3+}$ and $[Co(L)]^0$, which have the same absolute configuration, are linked by imidazole−imidazolate hydrogen bonds to form a puckered sheet structure with a trigonal void. Adjacent molecules with the same chirality are arrayed in an up-and-down fashion (Figure 1c). Sheets with the same chirality are stacked to give a homochiral crystal (conglomerate). Although the analogous perchlorate salt of the hemideprotonated complex, $[Co(H_{1.5}L)](ClO_4)_{1.5}\cdot 4H_2O$ ($=[Co^{III}(H_3L)][Co^{III}(L)](ClO_4)_3\cdot 8H_2O$, **2ClO₄**), consists of homochiral sheets, **2ClO₄** was found to be a racemic crystal; a homochiral sheet consisting of Δ enantiomers and an adjacent sheet consisting of Λ enantiomers stacked alternately to give a heterochiral crystal.[6]

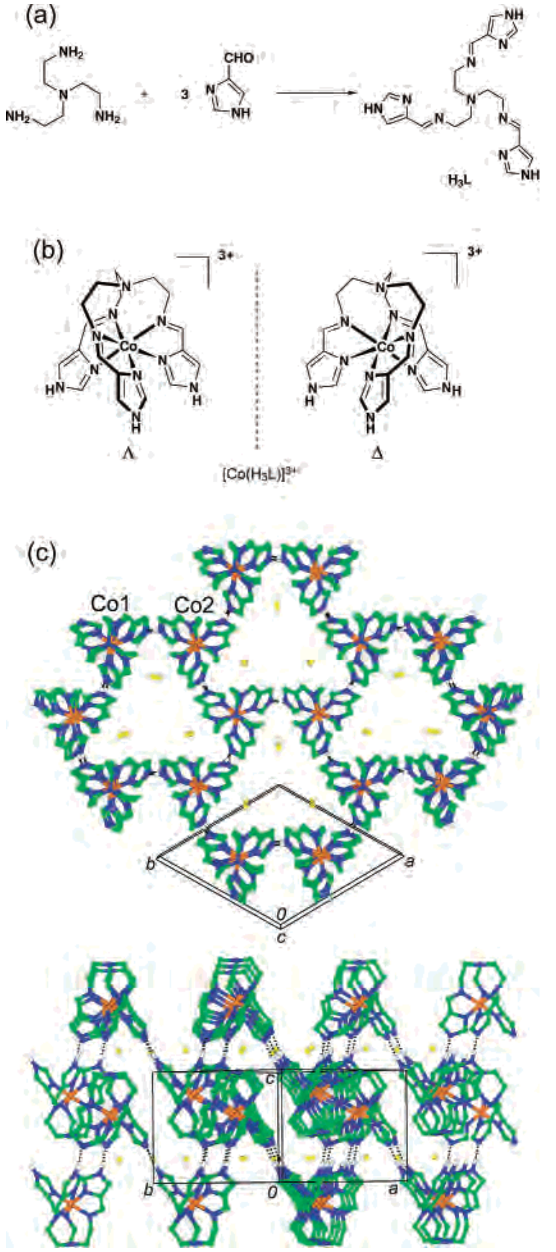

Figure 1. (a) Synthetic procedure for the tripodal H_3L ligand. (b) Δ and Λ configurations of $[Co(H_3L)]^{3+}$. (c) Top view (top) and side view (bottom) of the crystal structure of $[Co^{III}(H_{1.5}L)]Cl_{1.5}\cdot 4H_2O$ (i.e., $[Co^{III}(H_3L)][Co^{III}(L)]Cl_3\cdot 8H_2O$, **2Cl**), showing the 2D homochiral sheet formed by intermolecular hydrogen bonds between $[Co^{III}(H_3L)]^{3+}$ and $[Co^{III}(L)]^0$. The water molecules are omitted for clarity.

---

(3) (a) Jacques, J.; Collet, A.; Wilen S. H. *Enantiomers, Racemates and Resolutions*; Krieger Publishing Co.: Malabar, Florida, 1991. (b) Collet, A.; Brienne, M.-J.; Jacques, J. *Chem. Rev.* **1980**, *80*, 215−230.

(4) (a) Walba, D. M.; Körblova, E.; Shao, R.; Maclennan, J. E.; Link, D. R.; Glaser, M. A.; Clark, N. A. *J. Phys. Org. Chem.* **2000**, *13*, 830−836. (b) Weissbuch, I.; Kuzmenko, I.; Berfeld, L.; Leiserowitz, L.; Lahav, M. *J. Phys. Org. Chem.* **2000**, *13*, 426−434. (c) Yang, W.; Chai, X.; Chi, L.; Liu, X.; Cao, Y.; Lu, R.; Jiang, Y.; Tang, X.; Fuchs, H.; Li, T. *Chem.−Eur. J.* **1999**, *5*, 1144−1149.

(5) (a) Li, M.; Sun, Q.; Bai, Y.; Duan, C.; Zhang, B.; Meng, Q. *Dalton Trans.* **2006**, 2572−2578. (b) Li, F.; Li. T.; Li, X.; Li, X.; Wang, Y.; Cao, R. *Cryst. Growth Des.* **2006**, *6*, 1458−1462. (c) Gao, E.-Q.; Yue, Y.-F.; Bai, S.-Q.; He, Z.; Yan, C.-H. *J. Am. Chem. Soc.* **2004**, *126*, 1419−1429. (d) Tabellion, F. M.; Seidel, S. R.; Arif, A. M.; Stang, P. J. *Angew. Chem., Int. Ed.* **2001**, *40*, 1529−1532. (e) Yamaguchi, T.; Yamazaki, F.; Ito, T. *J. Am. Chem. Soc.* **2001**, *123*, 743−744. (f) Breu, J.; Domel, H.; Stoll, A. *Eur. J. Inorg. Chem.* **2000**, 2401−2408. (g) Krämer, R.; Lehn, J.-M.; De Cian, A.; Fischer, J. *Angew. Chem., Int. Ed. Engl.* **1993**, *32*, 703−706.

(6) Katsuki, I.; Motoda, Y.; Sunatsuki, Y.; Matsumoto, N.; Nakashima, T.; Kojima, M. *J. Am. Chem. Soc.* **2002**, *124*, 629−640.

(7) (a) Miyasaka, H.; Okamura, S.; Nakashima, T.; Matsumoto, N. *Inorg. Chem.* **1997**, *36*, 4329−4335. (b) Mimura, M.; Matsuo, T.; Motoda, Y.; Matsumoto, N.; Nakashima, T.; Kojima, M. *Chem. Lett.* **1998**, 691−692. (c) Katsuki, I.; Matsumoto, N.; Kojima, M. *Inorg. Chem.* **2000**, *39*, 3350−3354. (d) Kolks, G.; Frihart, C. R.; Rabinowitz, H. N.; Lippard, S. J. *J. Am. Chem. Soc.* **1976**, *98*, 5720−5721. (e) Matsumoto, N.; Motoda, Y.; Matsuo, T.; Nakashima, T.; Re, N.; Dahan, F.; Tuchagues, J.-P. *Inorg. Chem.* **1999**, *38*, 1165−1173. (f) Lorente, M. A. M.; Dahan, F.; Sanakis, Y.; Petrouleas, V.; Bousseksou, A.; Tuchagues, J.-P. *Inorg. Chem.* **1995**, *34*, 5346−5357. (g) Shii, Y.; Motoda, Y.; Matsuo, T.; Kai, F.; Nakashima, T.; Tuchagues, J.-P.; Matsumoto, N. *Inorg. Chem.* **1999**, *38*, 3513−3522. (h) Brewer, C. T.; Brewer, G.; Shang, M.; Scheidt, W. R.; Muller, I. *Inorg. Chim. Acta* **1998**, *278*, 197−201.

In both **2Cl** or **2ClO$_4$**, the counteranions are accommodated in a space between the sheets, and we suggested that the difference in size of the counteranion would affect the packing mode of the sheets. The importance of the counterion on conglomerate crystallization has been discussed for other chiral complexes.[8] For example, Yamanari et al.[8a] studied the solubility of the racemic and optically active isomers of $[Co(ox)(en)_2]X$ (X = Cl, Br, or I) and found out that the chloride and bromide salts crystallize as conglomerates, while the iodide salt gives a racemic crystal. It is to be noted that the iodide is also reported to crystallize in both of the monoclinic space groups *C*2 (conglomerate) and *C*2/*c* (racemate).[8c] In an effort to compare and to understand the conglomerate crystallization mechanism, Bernal et al.[8b−h] studied in detail the structures of several Co^{III} amine complexes. They proposed that the intra- and intermolecular hydrogen bonds, as well as the counteranion, play an essential role in conglomerate crystallization. To investigate the effect of the size and shape of the counteranion, we prepared a series of hemideprotonated complexes, $[Co(H_{1.5}L)]X_{1.5}\cdot nH_2O$ (X = Cl, Br, I, BF_4, ClO_4, and PF_6), and compared their crystal structures with each other. The optically active compound Λ-$[Co(H_{1.5}L)](ClO_4)_{1.5}\cdot H_2O$ (**Λ-2ClO$_4$**) was prepared from Λ-$[Co(H_3L)](ClO_4)_3\cdot 1.5H_2O$, and the crystal structure of **Λ-2ClO$_4$** was compared to that of the heterochiral crystal (***rac*-2ClO$_4$**).

Results and Discussion

Synthesis, Characterization, and Properties. The tripodal H_3L ligand was prepared by condensation reaction of tris(2-aminoethyl)amine and 4-formylimidazole in a 1:3 mole ratio in methanol (Figure 1). The ligand was not isolated, and a solution containing the ligand was allowed to react with *trans*-$[CoCl_2py_4]Cl$ (1:1) to yield $[Co(H_3L)]^{3+}$ (**1**). The complex was isolated as the perchlorate, $[Co(H_3L)](ClO_4)_3\cdot H_2O$ (**1ClO$_4$**). The uncoordinated NH groups of the imidazole moieties of the complex can be deprotonated by the action of a base. We have reported the preparation, structure, and properties of the fully deprotonated species, $[Co(L)]^0$, as well as **1ClO$_4$**.[6] The hemideprotonated species, $[Co(H_{1.5}L)]^{1.5+}$ (**2**), was prepared by adding a calculated amount (1.5 equiv) of a base to **1**. The chloride of the hemideprotonated complex, $[Co(H_{1.5}L)]Cl_{1.5}\cdot 4H_2O$ (**2Cl**), was prepared by adding a 1.5 equiv of triethylamine to a methanol solution of $[Co(H_3L)]Cl_3$, which was obtained by conversion of the perchlorate salt (**1ClO$_4$**) with an anion exchanger in the Cl^- form. $[Co(H_{1.5}L)]Br_{1.5}\cdot 4H_2O$ (**2Br**) was obtained by the addition of 1.5 equiv of NaOH and excess NaBr to an aqueous solution of $[Co(H_3L)]Cl_3$. Both $[Co(H_{1.5}L)](BF_4)_{1.5}\cdot 2.5H_2O$ (**2BF$_4$**) and $[Co(H_{1.5}L)](PF_6)_{1.5}\cdot 3.5H_2O$ (**2PF$_6$**) were prepared using the same method as for **2Br**, except that $NaBF_4$ and NH_4PF_6 were used instead of NaBr, respectively. The preparation of $[Co(H_{1.5}L)]I_{1.5}\cdot 2H_2O$ (**2I**) was not easy, because less soluble $[Co(H_{0.5}L)]I_{0.5}\cdot 4H_2O$ (**3I**) crystallized preferentially when a calculated amount (1.5 equiv) of NaOH and excess NaI were added to an aqueous solution of $[Co(H_3L)]Cl_3$. Thus, we added a smaller amount (1.4 equiv) of NaOH and obtained a mixture of $[Co(H_{0.5}L)]I_{0.5}\cdot 4H_2O$ (**3I**) and $[Co(H_{1.5}L)]I_{1.5}\cdot 2H_2O$ (**2I**). Since **2I** has a higher density ($D = 1.77$ g cm^{-3}) than **3I** ($D = 1.62$ g cm^{-3}), they were separated on the basis of the difference in density. The perchlorate of the optically active hemideprotonated complex, Λ-$[Co(H_{1.5}L)](ClO_4)_{1.5}\cdot H_2O$ (**Λ-2ClO$_4$**), was prepared by the addition of 1.5 equiv of NaOH and excess of $NaClO_4$ to an aqueous solution of Λ-$[Co(H_3L)]Cl_3$.

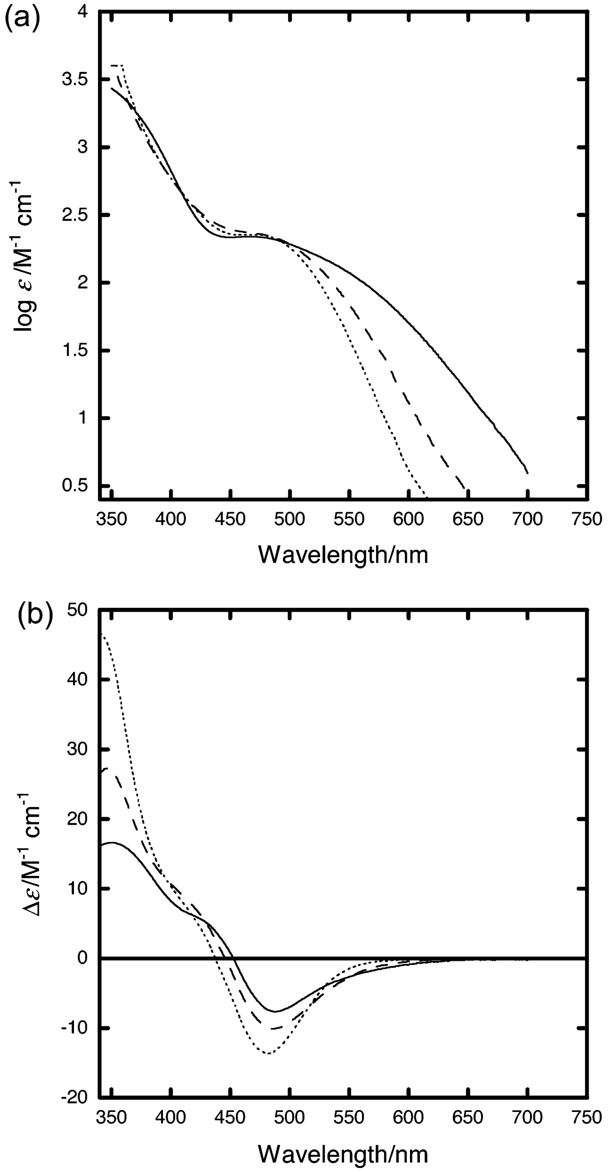

Figure 2. UV−vis and CD spectra of Λ-$[Co(H_{1.5}L)](ClO_4)_{1.5}\cdot H_2O$ (**Λ-2ClO$_4$**, dashed line), Λ-$[Co(H_3L)](ClO_4)_3\cdot 1.5H_2O$ (solid line), and Λ-$[Co(L)]$ (dotted line) in methanol.

All the hemideprotonated complexes showed two IR absorption bands in the 1592−1628 cm^{-1} region, which were assignable to the C=N stretching vibration of the tripodal

---

(8) (a) Yamanari, K.; Hidaka, J.; Shimura, Y. *Bull. Chem. Soc. Jpn.* **1973**, *46*, 3724−3728. (b) Bernal, I.; Cetrullo, J. *J. Coord. Chem.* **1989**, *20*, 259−265. (c) Bernal, I.; Cetrullo, J.; Myrczek, J.; Massoud, S. S. *J. Coord. Chem.* **1993**, *30*, 29−51. (d) Bernal, I.; Cetrullo, J.; Myrczek, J. *Mater. Chem. Phys.* **1993**, *35*, 290−300. (e) Bernal, I.; Cai, J.; Myrczek, J. *Polyhedron* **1993**, *12*, 1157−1162. (f) Bernal, I.; Myrczek, J.; Cai, J. *Polyhedron* **1993**, *12*, 1149−1155. (g) Bernal, I.; Jiwen, C.; Myrczek, J. *Polyhedron* **1993**, *12*, 1157−1162. (h) Saha, M.; Ramanujam, R.; Bernal, I.; Froncaek, F. R. *Cryst. Growth Des.* **2002**, *2*, 205−212.

Table 1. X-ray Crystallographic Data for $[Co(H_{1.5}L)]Br_{1.5}\cdot 4H_2O$ (**2Br**), $[Co(H_{1.5}L)]I_{1.5}\cdot 2H_2O$ (**2I**), $[Co(H_{1.5}L)](BF_4)_{1.5}\cdot 2.5H_2O$ (**2BF$_4$**), *rac*-$[Co(H_{1.5}L)](ClO_4)_{1.5}\cdot 4H_2O$ (***rac*-2ClO$_4$**), Λ-$[Co(H_{1.5}L)](ClO_4)_{1.5}\cdot H_2O$ (**Λ-2ClO$_4$**), $[Co(H_{1.5}L)](PF_6)_{1.5}\cdot 3.5H_2O$ (**2PF$_6$**), and $[Co(H_{0.5}L)]I_{0.5}\cdot 4H_2O$ (**3I**)

	2Br	**2I**	**2BF$_4$**
formula	$C_{18}H_{30.5}Br_{1.5}CoN_{10}O_4$	$C_{18}H_{26.5}CoI_{1.5}N_{10}O_2$	$C_{18}H_{27.5}B_{1.5}CoF_6N_{10}O_{2.5}$
fw	629.79	664.26	613.12
cryst system	trigonal	trigonal	trigonal
space group	*P*3 (No. 143)	*P*3 (No. 143)	*P*3 (No. 143)
a/Å	12.339(4)	12.388(3)	12.254(4)
b/Å	12.339(4)	12.388(3)	12.254(4)
c/Å	9.339(4)	9.389(3)	9.299(2)
α/deg	90	90	90
β/deg	90	90	90
γ/deg	120	120	120
V/Å^3	1231.4(7)	1247.8(5)	1209.2(6)
Z	2	2	2
D_{calc}/g cm^{-3}	1.698	1.768	1.684
μ/cm^{-1}	31.849	25.799	7.992
R_1	0.083 [$I > 2.0\sigma(I)$]	0.089 [$I > 2.0\sigma(I)$]	0.056 [$I > 2.0\sigma(I)$]
R_w	0.245 (all data)	0.265 (all data)	0.159 (all data)
T/°C	20	20	20
Flack param	0.05(3)	0.31(4)	0.24(2)

	***rac*-2ClO$_4$**[6]	**Λ-2ClO$_4$**
formula	$C_{18}H_{305}Cl_{1.5}CoN_{10}O_{10}$	$C_{18}H_{24.5}Cl_{1.5}CoN_{10}O_7$
fw	659.11	605.07
cryst system	monoclinic	trigonal
space group	*Cc* (No. 9)	*P*3 (No. 143)
a/Å	24.330(7)	12.304(4)
b/Å	12.887(5)	12.304(4)
c/Å	18.157(4)	9.315(3)
α/deg	90	90
β/deg	91.86(2)	90
γ/deg	90	120
V/Å^3	5690(3)	1221.2(6)
Z	8	2
D_{calc}/g cm^{-3}	1.539	1.645
μ/cm^{-1}	8.118	9.291
R_1	0.06 [$I > 2.0\sigma(I)$]	0.051 [$I > 2.0\sigma(I)$]
R_w	0.062 [$I > 2.0\sigma(I)$]	0.142 (all data)
T/°C	20	20
Flack param		0.10(2)

	2PF$_6$	**3I**
formula	$C_{18}H_{29.5}CoF_9N_{10}O_{3.5}P_{1.5}$	$C_{18}H_{29.5}CoI_{0.5}N_{10}O_4$
fw	718.38	572.38
cryst system	monoclinic	trigonal
space group	*C*2/*c* (No. 15)	$R\bar{3}c(h)$ (No. 167)
a/Å	25.096(6)	11.919(4)
b/Å	13.469(4)	11.919(4)
c/Å	17.884(4)	57.12(3)
α/deg	90	90
β/deg	91.545(8)	90
γ/deg	90	120
V/Å^3	6043(3)	7027(5)
Z	8	12
D_{calc}/g cm^{-3}	1.579	1.623
μ/cm^{-1}	7.446	14.395
R_1	0.066 [$I > 2.0\sigma(I)$]	0.026 [$I > 2.0\sigma(I)$]
R_w	0.185 (all data)	0.067 (all data)
T/°C	20	20
Flack param		

[a] $R_1 = \Sigma||F_o| - |F_c||/\Sigma|F_o|$. [b] $R_w = [\Sigma w(|F_o^2| - |F_c^2|)^2/\Sigma w|F_o^2|^2]^{1/2}$.

Schiff base ligand.[9] The IR spectra agreed with the crystal structures of the hemideprotonated complexes (vide infra) in that the complexes consist of two components, $[Co(H_3L)]^{3+}$ and [Co(L)]. We have shown that a complex with the ligand in the neutral form, H_3L, exhibits the ν(C═N) band in a higher wave number region than the deprotonated L^{3-} form does.[6,10] Thus, the bands at higher and at lower energy were assigned as the ν(C═N) bands of $[Co(H_3L)]^{3+}$ and [Co(L)], respectively.

Figure 2 shows the electronic and circular dichroism (CD) spectra of Λ-$[Co(H_{1.5}L)](ClO_4)_{1.5}\cdot H_2O$ (**Λ-2ClO$_4$**) in methanol, together with those of Λ-$[Co(H_3L)](ClO_4)_3\cdot 1.5H_2O$ and Λ-[Co(L)]. The first d−d absorption band of **Λ-2ClO$_4$**, $^1T_{1g} \leftarrow {}^1A_{1g}$ (O_h), is observed as a shoulder (λ = 480 nm, ϵ = 224 M^{-1} cm^{-1}) of an intense imine $\pi-\pi^*$ transition (λ =

---

(9) Nakamoto, K. *Infrared and Raman Spectra of Inorganic and Coordination Compounds*, 5th ed.; John Wiley and Sons: New York, 1997; Part B.

Table 2. Coordination Bond Distances (Å) for $[Co(H_{1.5}L)]Br_{1.5}\cdot 4H_2O$ (**2Br**), $[Co(H_{1.5}L)]I_{1.5}\cdot 2H_2O$ (**2I**), $[Co(H_{1.5}L)](BF_4)_{1.5}\cdot 2.5H_2O$ (**2BF$_4$**), *rac*-$[Co(H_{1.5}L)](ClO_4)_{1.5}\cdot 4H_2O$ (***rac*-2ClO$_4$**), Λ-$[Co(H_{1.5}L)](ClO_4)_{1.5}\cdot H_2O$ (**Λ-2ClO$_4$**), $[Co(H_{1.5}L)](PF_6)_{1.5}\cdot 3.5H_2O$ (**2PF$_6$**), and $[Co(H_{0.5}L)]I_{0.5}\cdot 4H_2O$ (**3I**)

	2Br	**2I**	**2BF$_4$**	**Λ-2ClO$_4$**		***rac*-2ClO$_4$**[6]
Co(1)−N(2)	1.970(5)	1.971(7)	1.964(11)	1.976(3)		1.90(2)
Co(1)−N(3)	1.894(4)	1.902(5)	1.910(12)	1.902(2)		1.92(2)
Co(1)−N(5)						1.88(2)
Co(1)−N(6)						1.92(2)
Co(1)−N(8)						1.98(2)
Co(1)−N(9)						1.88(2)
Co(2)−N(6)	1.972(4)	1.974(7)	1.970(10)	1.967(3)	Co(2)−N(12)	1.931(19)
Co(2)−N(7)	1.895(6)	1.901(5)	1.901(11)	1.910(3)	Co(2)−N(13)	1.927(16)
					Co(2)−N(15)	1.99(2)
					Co(2)−N(16)	1.863(15)
					Co(2)−N(18)	2.03(2)
					Co(2)−N(19)	1.886(16)

	2PF$_6$	**3I**
Co(1)−N(2)	1.950(3)	1.9769(19)
Co(1)−N(3)	1.912(3)	1.9064(15)
Co(1)−N(5)	1.959(3)	
Co(1)−N(6)	1.909(3)	
Co(1)−N(8)	1.946(3)	
Co(1)−N(9)	1.894(3)	

ca. 320 nm, $\epsilon = 5000\ M^{-1}\ cm^{-1}$), which hides the weak second d−d absorption band, ${}^1T_{2g} \leftarrow {}^1A_{1g}$ (O_h).[11] **Λ-2ClO$_4$** exhibits a negative CD band in the first d−d absorption band region ($\lambda = 486$ nm, $\Delta\epsilon = -10.1\ M^{-1}\ cm^{-1}$). As expected, the UV−vis and CD spectral features of **Λ-2ClO$_4$** are between those of Λ-$[Co(H_3L)](ClO_4)_3\cdot 1.5H_2O$ and Λ-[Co(L)].[12]

In a previous paper,[6] we reported that $[Co(H_{1.5}L)]Cl_{1.5}\cdot 4H_2O$ (**2Cl**) crystallizes as a conglomerate, while $[Co(H_{1.5}L)](ClO_4)_{1.5}\cdot 4H_2O$ (**2ClO$_4$**), as a racemic crystal. We have measured the CD spectra of crystallites of the hemideprotonated complexes to examine if they crystallized as conglomerates. A crystallite of **2Br** was dissolved in dimethyl sulfoxide, and the spectrum was measured in the range $\lambda = 330{-}600$ nm. The spectrum showed a negative and a positive peak at 486 and 347 nm, respectively, and the spectrum of another crystallite showed an enantiomeric CD pattern, demonstrating that **2Br** crystallized as a conglomerate. We have confirmed that **2Br**, **2I**, and **2BF$_4$** crystallized as conglomerates, while **2PF$_6$** and **2ClO$_4$** did not (see Supporting Information Figure S1). The results are in agreement with the X-ray structural analysis.

X-ray Crystal Structures. The crystal data for **2Br**, **2I**, **2PF$_6$**, ***rac*-2ClO$_4$**, **Λ-2ClO$_4$**, and **3I** are summarized in Table 1. Although the H_3L ligand is potentially heptadentate,[13] the tertiary amine nitrogen atom is not coordinated to the metal atom, (the N(tertiary amine)⋯Co distance being 3.33−3.44 Å) and the ligand serves as a hexadentate ligand in these complexes. In each complex, three imine (Schiff base) nitrogen atoms and three imidazole nitrogen atoms are coordinated to form an octahedral Co^{III} complex. The relevant coordination bond distances are listed in Table 2. Each complex is chiral, with either a Δ (clockwise) or a Λ (anticlockwise) configuration, due to the screw coordination arrangement of the tripodal ligand around the Co^{III} ion. As described above, **2Br**, **2I**, and **2BF$_4$** crystallize as conglomerates, and **Λ-2ClO$_4$** was derived from Λ-$[Co(H_2L)][Sb_2((R,R)\text{-tart})_2]\cdot 4H_2O$. The absolute configurations of the chiral crystals **2Br**, **2I**, **2BF$_4$**, and **Λ-2ClO$_4$**, which were subjected to the X-ray analysis, were determined using the Flack parameters.[14]

Structure of $[Co(H_{1.5}L)]Br_{1.5}\cdot 4H_2O$ (2Br) and $[Co(H_{1.5}L)]I_{1.5}\cdot 2H_2O$ (2I). **2Br** crystallized in the trigonal space group *P*3 (No. 143), with $Z = 2$. The crystal structure consists of one $[Co(H_3L)]^{3+}$ cation, one neutral [Co(L)] species, three Br^- ions, and eight water molecules (seven molecules with occupancy (Occ) = 1, and three molecules with Occ = 1/3) as the unique unit. Figure 3 shows the ORTEP drawings of $[Co(H_3L)]^{3+}$ and [Co(L)] along with the selected numbering scheme. The crystal structure of **2Br** is similar to that of **2Cl**.[6] Figure 4a,b shows a top and a side view of **2Br**, respectively. Component species with the same Δ configuration are linked by imidazole−imidazolate hydrogen bonds with an N(4)⋯N(8) distance of 2.716(8) Å to form a puckered 2D sheet composed of a hexanuclear unit with a trigonal void in the *ab*-plane (shown by the green triangle in Figure 4). Sheets with the same chirality are stacked along the *c*-axis to form a chiral crystal, as evidenced by the CD spectrum (see Supporting Information Figure S1). The three Br^- ions are coplanar in the *ab*-plane, and they are located

---

(10) (a) Ikuta, Y.; Ooidemizu, M.; Yamahata, Y.; Yamada, M.; Osa, S.; Matsumoto, N.; Iijima, S.; Sunatsuki, Y.; Kojima, M.; Dahan, F.; Tuchagues, J.-P. *Inorg. Chem.* **2003**, *42*, 7001−7017. (b) Yamada, M.; Ooidemizu, M.; Ikuta, Y.; Osa, S.; Matsumoto, N.; Iijima, S.; Kojima, M.; Dahan, F.; Tuchagues, J.-P. *Inorg. Chem.* **2003**, *42*, 8406−8416. (c) Sunatsuki, Y.; Ohta, H.; Kojima, M.; Ikuta, Y.; Goto, Y.; Matsumoto, N.; Iijima, S.; Akashi, H.; Kaizaki, S.; Dahan, F.; Tuchagues, J.-P. *Inorg. Chem.* **2004**, *43*, 4154−4171.

(11) (a) Tanabe, Y.; Sugano, S. *J. Phys. Soc. Jpn.* **1954**, *9*. 753−766. (b) Lever, A. B. P. *Inorganic Electronic Spectroscopy*; Elsevier: Amsterdam, 1968.

(12) Nakamura, H.; Fujii, M.; Sunatsuki, Y.; Kojima, M.; Matsumoto, N. Manuscript in preparation.

(13) Brewer, C.; Brewer, G.; Butcher, R. J.; Carpenter, E. E.; Cuenca, L.; Noll, B. C.; Scheidt, W. R.; Viragh, C.; Zavalij, P. Y.; Zielaski, D. *Dalton Trans.* **2006**, 1009−1019.

(14) Flack, H. D. *Acta Crystallogr., Sect. A* **1993**, *39*, 876−881.

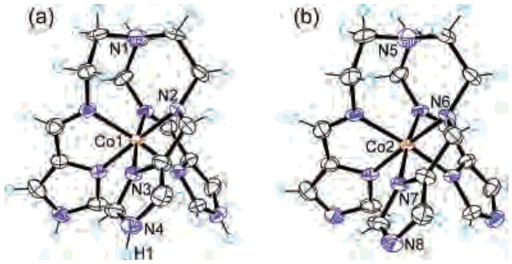

Figure 3. ORTEP drawings of (a) $[Co(H_3L)]^{3+}$ and (b) [Co(L)] in $[Co(H_{1.5}L)]Br_{1.5}\cdot 4H_2O$ (**2Br**) with their selected numbering schemes. Both component species have the same absolute configuration (Δ).

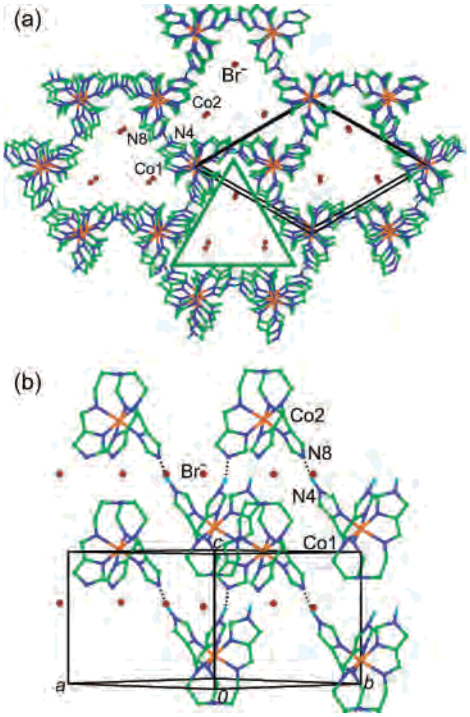

Figure 4. Crystal structure of $[Co(H_{1.5}L)]Br_{1.5}\cdot 4H_2O$ (**2Br**). Water molecules and the hydrogen atoms, except for that attached to N4, have been omitted for clarity. Component species with the same Δ configuration are linked by imidazole−imidazolate hydrogen bonds. (a) Top view of the homochiral 2D-sheet structure formed by hydrogen bonds between the molecules. A trigonal void formed by a hexanuclear unit is shown by the green triangle. (b) Side view showing the up-and-down molecular array.

in a trigonal homochiral channel. The Br···Br distance is 5.663 Å, which is smaller than the Cl···Cl distance (5.756 Å) in **2Cl**. The water molecules are located deeper in the triangular channel than the Br^- ions are.

2I also crystallizes in the acentrosymmetric trigonal space group *P*3 (No. 143), with $Z = 2$. The crystal structure consists of one $[Co(H_3L)]^{3+}$ cation, one neutral [Co(L)] species, three I^- ions, and four water molecules (six molecules with Occ = 1/2 and three molecules with Occ = 1/3) as the unique unit. The overall crystal structure is very similar to those of **2Cl** and **2Br** (see Supporting Information Figure S2). The component species are linked by N(4)···N(8) hydrogen bonds with a distance of 2.719(1) Å. Here again, the I^- ions are accommodated in the intermediate region of the double layer, and they are in the triangular chiral channel. The I···I distance is 5.412 Å, and the I^- ions are closer to the center of the channel than the Cl^- and Br^- ions are in **2Cl** and **2Br**, respectively.

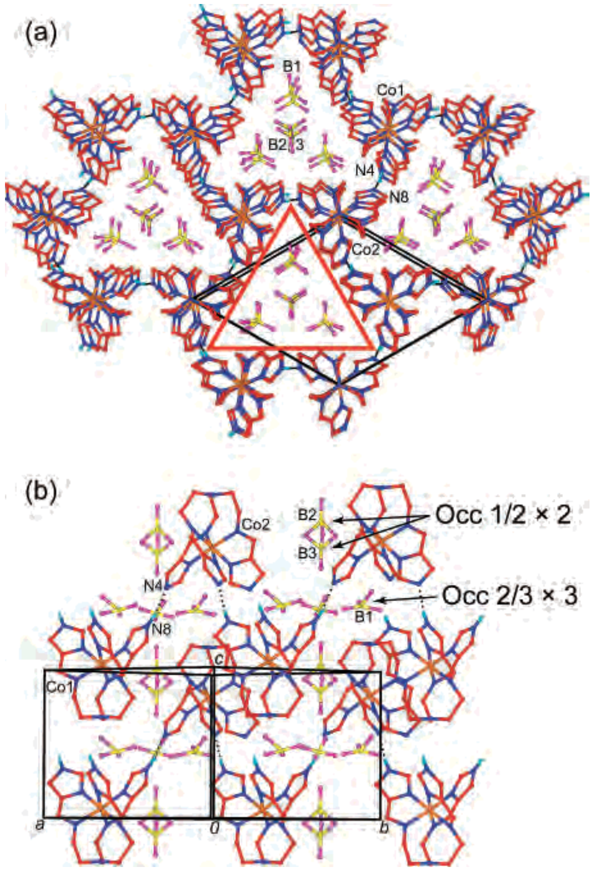

Figure 5. Crystal structure of $[Co(H_{1.5}L)](BF_4)_{1.5}\cdot 2.5H_2O$ (**2BF₄**). Water molecules and the hydrogen atoms, except for those attached to N4, have been omitted for clarity. The component species, $[Co(H_3L)]^{3+}$ and $[Co^{III}(L)]$, have the same Λ absolute configuration. (a) Top view of the homochiral 2D-sheet structure formed by hydrogen bonds between the molecules. A trigonal void formed by a hexanuclear unit is shown by the red triangle. (b) Side view showing the up-and-down molecular array. There are two types of BF_4^- ion: Two ions (B(1), Occ = 2/3 × 3) are accommodated in the intermediate region of the double layer, and the remainder (B(2) and B(3), Occ = 1/2 × 2) are on the crystallographic C_3 axis, with all anions being located in the channel.

Structure of $[Co(H_{1.5}L)](BF_4)_{1.5}\cdot 2.5H_2O$ (2BF₄). **2BF₄** also crystallized as a conglomerate in the acentrosymmetric trigonal space group *P*3 (No. 143), with $Z = 2$. The overall crystal structure is similar to those of **2Cl**, **2Br**, and **2I** (Figure 5). The crystal structure consists of one $[Co(H_3L)]^{3+}$ cation, one neutral [Co(L)] species, three BF_4^- ions, and five water molecules (one molecule with Occ = 1 and 12 molecules with Occ = 1/3) as the unique unit. The N(4)···N(8) hydrogen bond distance connecting the two components is 2.739(18) Å. The crystal subjected to the X-ray structural analysis consisted of component species with the same Λ configuration. There are two types of BF_4^- ion: Two ions (B(1), Occ 2/3 × 3) are accommodated in the intermediate region of the double layer as halide ions in **2Cl**, **2Br**, and **2I**, and the remainder (B(2) and B(3), Occ 1/2 × 2) are on the crystallographic C_3 axis. All anions are located in the trigonal channel comprised of six complexes. The B(1)···B(1) distance is 5.052 Å, with this value being smaller than

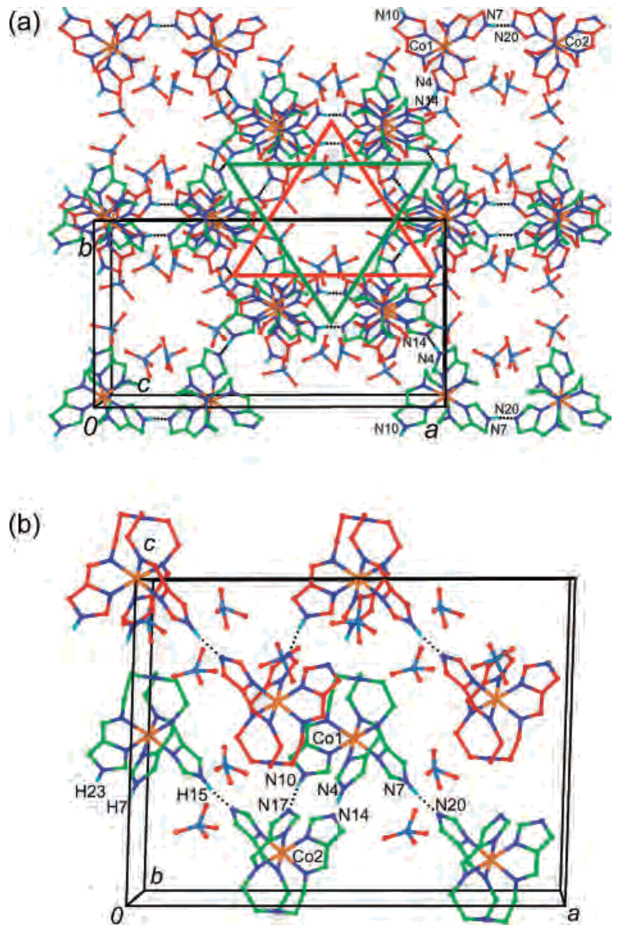

Figure 6. Crystal structure of *rac*-[Co($H_{1.5}$L)](ClO_4)$_{1.5}$·4H_2O (***rac*-2ClO$_4$**). Water molecules and the hydrogen atoms, except for those attached to N4, N7, and N10, have been omitted for clarity. The carbon atoms of the Δ and Λ enantiomers are shown in green and red, respectively. The triangles denote the trigonal voids formed by hexanuclear units. (a) Top view showing that two components with the same absolute configuration, [Co(H_3L)]$^{3+}$ and [Co(L)], are linked by hydrogen bonds to form a homochiral 2D-sheet structure. (b) Side view showing the up-and-down molecular array. The ClO_4^- ions are not in the same *ab*-plane. They are accommodated in the heterochiral channel formed by stacking of the Δ and Λ double layers with a trigonal void along the *c*-axis.

those of the $X^- \cdots X^-$ (where X = Cl, Br, and I) distances, and thus, the BF_4^- ions are closer to the center of the chiral trigonal channel than are the halide ions. There are three types of water molecules: O(1) is located at the center of the three B(1) atoms, O(2) and O(3) (Occ = 1/3 × 6) are located at the same position as the B(1) atoms, and O(4) and O(5) (Occ = 1/3 × 6) are positioned above and below the B(1) atoms.

Structure of *rac*-[Co($H_{1.5}$L)](ClO_4)$_{1.5}$·4H_2O (*rac*-2ClO$_4$) and Λ-[Co($H_{1.5}$L)](ClO_4)$_{1.5}$·H_2O (Λ-2ClO$_4$). 2ClO$_4$ does not undergo conglomerate crystallization, and we have previously reported its crystal structure.[6] This crystallizes in the monoclinic space group *Cc* (No. 9), with *Z* = 8. The crystal structure consists of one [Co(H_3L)]$^{3+}$ cation, one neutral [Co(L)] species, three ClO_4^- ions (two ions with Occ = 1 and two ions with Occ = 1/2), and eight water molecules as the unique unit. The two component molecules with the same absolute configuration are linked by hydrogen bonds with distances of N(4)···N(14) = 2.72(2), N(10)···N(17) = 2.69(3), and N(7)···N(20) = 2.70(2) Å, to give a homochiral double layer structure. A homochiral sheet consisting of Δ enantiomers and an adjacent sheet consisting of Λ enantiomers are stacked alternately to give a heterochiral structure (Figure 6). The trigonal void formed by the Δ enantiomers (shown by the green triangle in Figure 6a) and that formed by the Λ components (shown by the red triangle in Figure 6a) form in the opposite direction. The counteranions are not on in the same *ab*-plane as are the halide ions in **2Cl**, **2Br**, and **2I**. They are accommodated in the heterochiral channel comprised of a stacking of the Δ and Λ double layers with a trigonal void along the *c*-axis (vide infra). The water molecules are located in the channels inside the anions. The skeletal structure of ***rac*-2ClO$_4$** is more flattened and spread out in the *ab*-plane, especially along the *a*-axis than in **2Cl**, **2Br**, and **2I**, and there is a small shift along the *b*-axis direction. These structural features will be discussed in more detail later.

The structure of optically active Λ-[Co($H_{1.5}$L)](ClO_4)$_{1.5}$·H_2O (**Λ-2ClO$_4$**) is similar to that of [Co($H_{1.5}$L)](BF_4)$_{1.5}$·2.5H_2O (**2BF$_4$**). **Λ-2ClO$_4$** crystallizes in the acentrosymmetric trigonal space group *P*3 (No. 143), with *Z* = 2. The crystal structure consists of one [Co(H_3L)]$^{3+}$ cation, one neutral [Co(L)] species, three ClO_4^- ions (three ions with Occ = 2/3 and two ions with Occ = 1/2), and two water molecules (one molecule with Occ = 1 and three molecules with Occ = 1/3) as the unique unit. Component species are linked by N(4)···N(8) hydrogen bonds with a distance of 2.748(4) Å to produce a puckered 2D sheet structure. Such sheets stack along the *c*-axis to form a homochiral crystal (Figure 7). There are two types of ClO_4^- ion: Two ions (Cl(1), Occ = 2/3 × 3) are accommodated in the intermediate region of the double layer as halide ions in **2Cl**, **2Br**, and **2I**, the remainder (Cl(2) and Cl(3), Occ = 1/2 × 2) are along the crystallographic C_3 axis, and all anions are located in the trigonal homochiral channel. These features regarding the positions of counterions are similar to those of **2BF$_4$**. The Cl(1)···Cl(1) distance is 5.138 Å, and this value is a little larger than the B···B distance in **2BF$_4$** (5.035 Å).

Structure of [Co($H_{1.5}$L)](PF_6)$_{1.5}$·3.5H_2O (2PF$_6$). Although the IR spectrum indicated the presence of two components, [Co(H_3L)]$^{3+}$ and [Co(L)], the X-ray crystallographic data could not differentiate these. The Occ value of the hydrogen atom for the uncoordinated imidazole NH group was Occ = 1/2, and the space group was not *Cc*, as in ***rac*-2ClO$_4$**, but was the more symmetrical *C*2/*c*. Thus, the X-ray structure we analyzed showed only the average structure of the [Co(H_3L)]$^{3+}$ and [Co(L)] forms. The crystal structure consisted of one [Co($H_{1.5}$L)]$^{1.5+}$ cation, one and a half PF_6^- ions (one anion with Occ = 1 and one anion with Occ = 1/2), and three and a half water molecules (three molecules with Occ = 1 and one molecule with Occ = 1/2) as the unique unit. The two component molecules are linked by hydrogen bonds, N(4)···N(10) = 2.734(5), N(7)···N(7) = 2.689(4), and N(10)···N(4) = 2.734(5) Å, to give a homochiral double layer structure in the *ab*-plane. A homochiral puckered sheet consisting of Δ enantiomers and an adjacent sheet consisting of Λ enantiomers are stacked

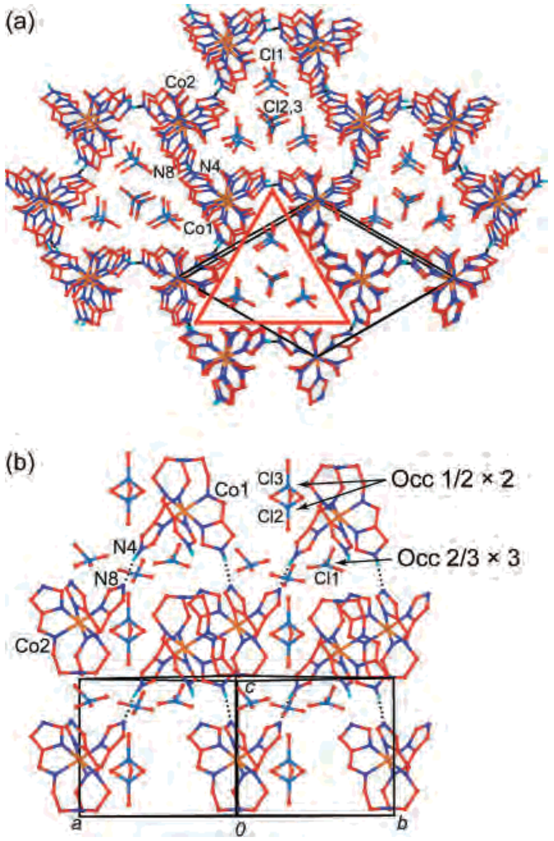

Figure 7. Crystal structure of Λ-[Co($H_{1.5}L$)]$(ClO_4)_{1.5}$·H_2O (**Λ-2ClO₄**). Water molecules and the hydrogen atoms, except for that attached to N4, have been omitted for clarity. (a) Top view of the homochiral 2D-sheet structure formed by hydrogen bonds between the molecules. A trigonal void formed by a hexanuclear unit is shown by the red triangle. (b) Side view showing the up-and-down molecular array. There are two types of ClO_4^- ions: Two ions (Cl(1), Occ = 2/3 × 3) are accommodated in the intermediate region of the double layer, and the remainder (Cl(2) and Cl(3), Occ = 1/2 × 2) are on the crystallographic C_3 axis. All anions are located in the trigonal channel comprised of six complexes.

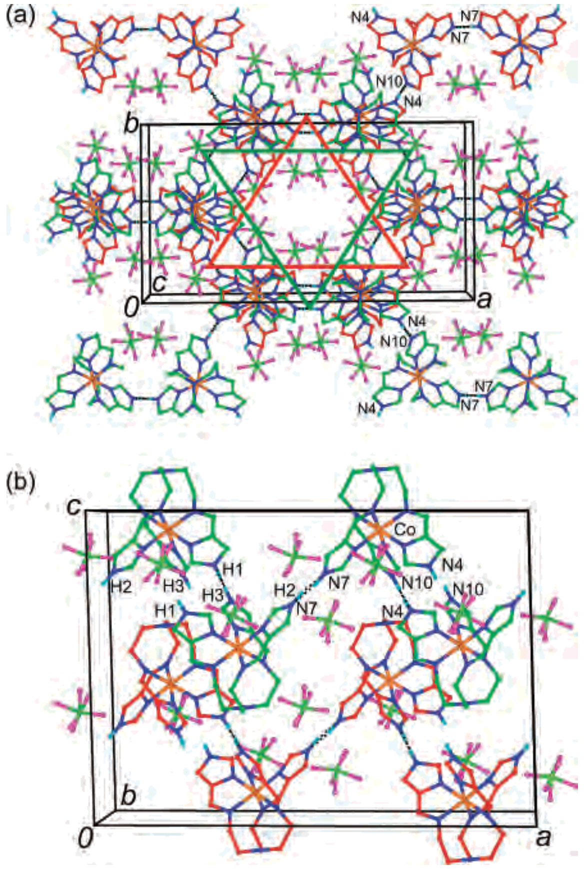

Figure 8. Crystal structure of [Co($H_{1.5}L$)]$(PF_6)_{1.5}$·3.5H_2O (**2PF₆**). Water molecules and the hydrogen atoms, except for those attached to N4, N7, and N10 have been omitted for clarity. The carbon atoms of the Δ and Λ enantiomers are shown in green and red, respectively. (a) Top view showing that two components with the same absolute configuration, $[Co(H_3L)]^{3+}$ and [Co(L)], are linked by hydrogen bonds to form a homochiral 2D-sheet structure. The triangles denote trigonal voids formed by hexanuclear units. (b) Side view showing the up-and-down molecular array. The counteranions are not in the *ab*-plane and are accommodated in the channels comprised of stacks of two types of double layers.

alternately to give a heterochiral structure, as in ***rac*-2ClO₄** (Figure 8). The counteranions are not in the *ab*-plane and are accommodated in the heterochiral channel. The situation is again similar to that of ***rac*-2ClO₄**. We will discuss this in more detail in a later section.

Structure of [Co($H_{0.5}L$)]$I_{0.5}$·4H_2O (3I). This complex was obtained as a byproduct of [Co($H_{1.5}L$)]$I_{1.5}$·2H_2O (**2I**). **3I** crystallized in the trigonal space group $R\bar{3}c$(*h*) (No. 167), with $Z = 12$. The crystal structure consists of one $[Co(H_{0.5}L)]^{0.5+}$ cation, half an I^- ion, and four water molecules as the unique unit. A heterochiral 2D sheet structure is constructed by hydrogen bonds between the imidazole (or imidazolate) groups and the water of crystallization with an N(4)···O(2) distance of 2.775(2) Å and between the water of crystallization molecules with the distances of O(1)···O(2) = 2.825(2) Å and O(2)···O(2) = 2.881(2) Å (Figures 9 and 10). The occupancy of the H atoms of the uncoordinated imidazole NH group is 1/6, and the I^- ion resides at the center of the space comprised of six complex cations. The hydrogen atoms attached to O1 are disordered. The Occ value of the H atoms on the C_3 axis is Occ = 1, while that of the other three H atoms is Occ = 1/3. The double-layer sheets are stacked adjacent to each other, so that they fill out the space, and there is no interaction between the sheets (Figure 9).

Comparison of the Homochiral and Heterochiral Crystals of the Hemideprotonated Complexes. In the crystal of a hemideprotonated complex, two components with the same absolute configuration, $[Co(H_3L)]^{3+}$ and [Co(L)], are linked by imidazole−imidazolate hydrogen bonds to form an extended 2D sheet structure having a hexanuclear unit with a trigonal void in the *ab*-plane. There are two alternative stacking options for these homochiral sheets along the *c*-axis. When adjacent homochiral sheets with the same chirality are stacked, a chiral crystal is formed. On the other hand, when a homochiral sheet with Δ enantiomers and an adjacent homochiral layer with Λ enantiomers are stacked alternately, a heterochiral crystal is formed. In either case, counteranions and water of crystallization molecules are accommodated in the channels. The channel shape depends on the stacking mode of the sheets: a homochiral crystal has a straight channel, because the sheets are stacked along the *c*-axis without any shift (Figure 11a). An achiral crystal has a zigzag channel along the *c*-axis, and the channel can adopt the

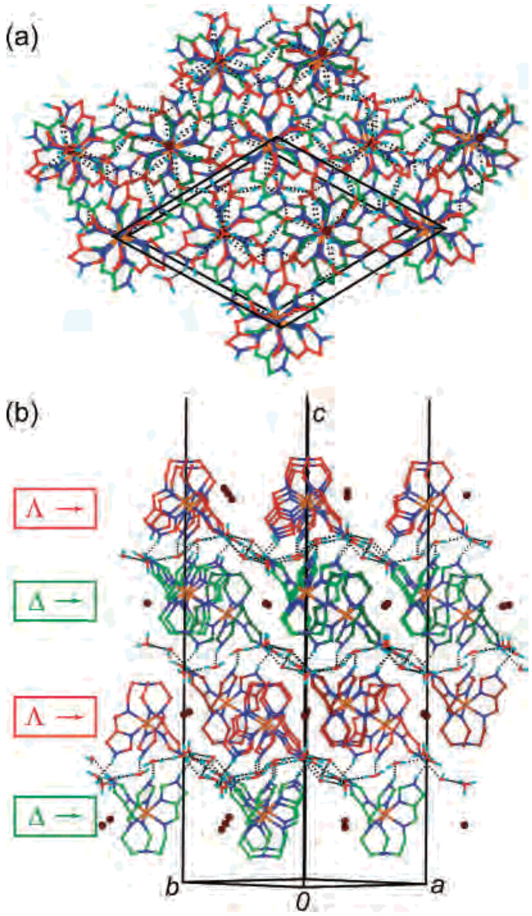

Figure 9. (a) Top view and (b) side view of the crystal structure of [Co-($H_{0.5}L$)]$I_{0.5}$·4H_2O (**3I**). The heterochiral 2D sheet structure is constructed by hydrogen bonds between imidazole (or imidazolate) and the water of crystallization and between the water of crystallization molecules. The carbon atoms of the Δ and Λ enantiomers are shown in green and red, respectively. The sheets are stacked each other so that they fill out the space, and there is no interaction between the sheets.

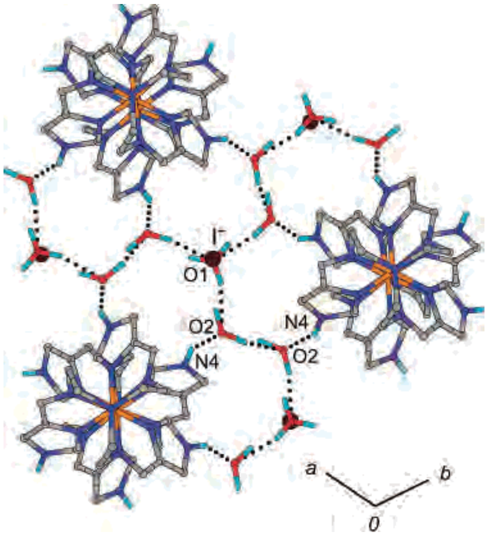

Figure 10. Intermolecular hydrogen bonding in [Co($H_{0.5}L$)]$I_{0.5}$·4H_2O (**3I**). The I^- ion resides at the center of the space comprised of six complex cations.

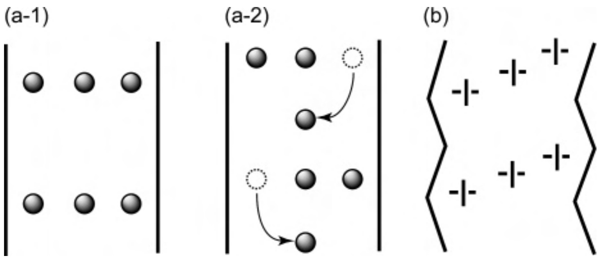

Figure 11. Schematic illustration of two types of channel shape: (a) a straight channel (a-1) in a chiral crystal, where the halide ions of **2Cl**, **2Br**, and **2I** are in the *ab*-plane, and (a-2) in the crystals of **2BF$_4$** and **Λ-2ClO$_4$**, where three counterions cannot reside in the same plane due to steric congestion and one of the ions is pushed onto the crystallographic C_3 axis; (b) a zigzag channel in a heterochiral crystal (racemic crystal), as observed in ***rac*-2ClO$_4$** and **2PF$_6$**, where the counteranions are situated obliquely to the *ab*-plane and the anions can avoid steric congestion occurring.

counteranions obliquely in the *ab*-plane so that the anions can avoid steric congestion occurring between them (Figure 11b). There are two ways of accommodating the counterions in the homochiral channels (Figure 11a-1,a-2). In the crystals of **2Cl**, **2Br**, and **2I** with relatively small ions (ionic radius $r(Cl^-) = 1.67$ Å, $r(Br^-) = 1.82$ Å, and $r(I^-) = 2.06$ Å),[15] the halide ions are in the *ab*-plane in a channel (Figure 11a-1). The X···X distance decreases in the following order: Cl···Cl (5.756 Å) > Br···Br (5.663 Å) > I···I (5.412 Å). Thus, the steric interaction between the anions seems to be less important than that between the skeleton and the anions in these complexes. When the size of the anion increases, the anions assume a different arrangement in the channels. In the crystal of **2BF$_4$** ($r(BF_4^-) = 2.84$ Å),[15] the three counterions cannot reside in the same plane due to the steric congestion; one of the ions is pushed into the crystallographic C_3 axis (Figure 11a-2), and the position that may have been occupied by a BF_4^- ion is filled with a water molecule (Occ = 1/3, Figure 5). In the crystal of **Λ-2ClO$_4$** ($r(ClO_4^-) = 2.90$ Å),[15] the positions of the three ClO_4^- ions are almost the same as those of the BF_4^- ions in **2BF$_4$** (Figure 7). The steric interaction between the anions is higher in **Λ-2ClO$_4$**, resulting in a longer Cl(1)···Cl(1) distance (5.138 Å) than B(1)···B(1) distance (5.052 Å). It should be noted that **2ClO$_4$** does not undergo conglomerate crystallization and that **Λ-2ClO$_4$** was obtained from Λ-[Co(H_3L)]-(ClO_4)$_3$·1.5H_2O.

The difference in ionic size between BF_4^- (2.84 Å) and ClO_4^- (2.90 Å) ions is small. However, this difference has a pronounced effect: **2BF$_4$** gives a conglomerate, whereas **2ClO$_4$** forms a heterochiral crystal. A heterochiral crystal (racemic crystal) affords a zigzag channel, where large counteranions can be accommodated (Figure 11 b), and therefore, it is natural that **2PF$_6$** with large anions ($r(PF_6^-) = 3.01$ Å)[15] gives a heterochiral crystal.

Table 3 shows a comparison of the intersheet Co···Co distances and two types of intrasheet Co···Co distances. One is for Co···Co bridged by NH···N hydrogen bonds, and the other is for next neighbor Co···Co (see Figure 12 for definition).

---

(15) (a) Weast, R. C., Ed. *Handbook of Chemistry and Physics*; CRC Press: Boca Raton, FL, 1980. (b) Peulon, V.; Barbey, G.; Malandain, J.-J. *Synth. Met.* **1996**, *82*, 111−117. (c) Shannon, R. D. *Acta Crystallogr.* **1976**, *A32*, 751−767. (d) Shannon, R. D.; Prewitt, C. T. *Acta Crystallogr.* **1969**, *B25*, 925−946.

Table 3. Intersheet Co···Co Distances and Two Kinds of Intrasheet Co···Co Distances (Å) of Hemideprotonated Complexes $[Co(H_{1.5}L)]Cl_{1.5}\cdot 4H_2O$ (**2Cl**), $[Co(H_{1.5}L)]Br_{1.5}\cdot 4H_2O$ (**2Br**), $[Co(H_{1.5}L)]I_{1.5}\cdot 2H_2O$ (**2I**), $[Co(H_{1.5}L)](BF_4)_{1.5}\cdot 2.5H_2O$ (**2BF₄**), *rac*-$[Co(H_{1.5}L)](ClO_4)_{1.5}\cdot 4H_2O$ (***rac*-2ClO₄**), Λ-$[Co(H_{1.5}L)](ClO_4)_{1.5}\cdot H_2O$ (**Λ-2ClO₄**), and $[Co(H_{1.5}L)](PF_6)_{1.5}\cdot 3.5H_2O$ (**2PF₆**)

	2Cl	**2Br**	**2I**	**2BF₄**	**Λ-2ClO₄**	***rac*-2ClO₄**[6]	**2PF₆**
intersheet Co···Co dist[a]	9.321	9.339	9.389	9.3	9.315	9.1	9.016
intrasheet Co···Co dist, bridged by NH···N hydrogen bonds[a]	10.404	10.395	10.431	10.392	10.4	10.382	10.491
next-neighbor Co···Co dist in a sheet[a]	12.277	12.339	12.388	12.254	12.304	12.887 13.766 13.766 (av. 13.473)	13.469 14.241 14.241 (av. 13.984)

[a] See Figure 12 for definition.

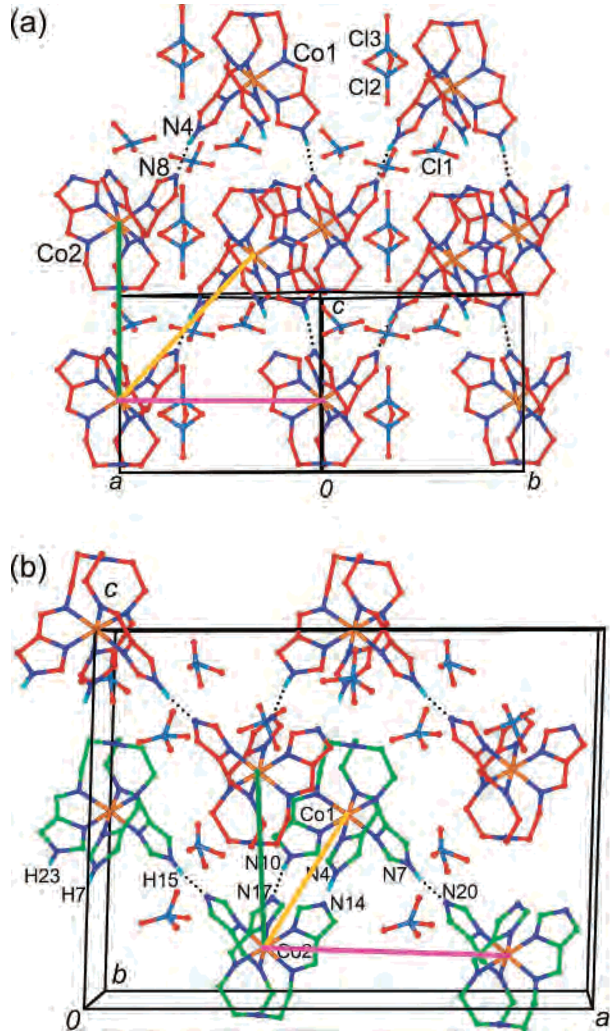

Figure 12. Three types of Co···Co distances: (a) in a homochiral crystal, **Λ-2ClO₄**; (b) in a heterochiral crystal, ***rac*-2ClO₄**. These are the intersheet Co···Co distance (shown by the green line), the intrasheet Co···Co distance bridged by NH···N hydrogen bonds (shown by the orange line), and the next-neighbor intrasheet Co···Co distance (shown by the purple line).

The following trends are observed from the data:

(1) The homochiral crystals have larger intersheet Co···Co distances (≥9.3 Å) than the heterochiral Co···Co distances (≤9.1 Å). The Co···Co distance is larger for *rac*-$2ClO_4$ (9.1 Å) than for $2PF_6$ (9.0 Å).

(2) The intrasheet Co···Co bond distances bridged by NH···N hydrogen bonds are about 10.4 Å, irrespective of the counteranion.

(3) The next-neighbor intrasheet Co···Co distances are longer for the heterochiral crystals than for the homochiral crystals. A comparison of the two heterochiral crystals **2PF₆** and ***rac*-2ClO₄** reveals that the former has a longer distance (average = 13.984 Å) than the latter (average = 13.473 Å).

In summary, the heterochiral crystals have a more spread out and flattened structure in the *ab*-plane than the homochiral crystals do, and moreover, **2PF₆** with large counteranions ($r(PF_6^-)$ = 3.01 Å) has a more spread out structure than ***rac*-2ClO₄** does ($r(ClO_4^-)$= 2.90 Å). It should be noted that the skeletal structure of the homochiral crystals is not affected by the type of counteranion. The heterochiral crystals do not have a crystallographic C_3 axis of symmetry, and the degree of spreading out is different between the *a*- and *b*-axial directions. The spreading out along the *a*-axis affords a larger space for accommodating larger counteranions. Although the spreading out along the *b*-axis is not as large as in the *a*-axis direction, a large space is formed by stacking the sheets with a shift, as shown in Figures 11 and 13, and this shift is larger in **2PF₆** (0.858 Å) with large counteranions than it is in ***rac*-2ClO₄** (0.538 Å). Since the 2D skeletal structure of the heterochiral crystals can spread out and flatten, we conclude that the heterochiral structure is much more flexible than is the homochiral structure.

Table 4 shows a comparison of the size of the void in the homochiral and heterochiral crystals. Here, the void is defined by the triangle formed by connecting the imidazole H(1) atoms (Figures 4−8). The heterochiral **2PF₆** complex has the largest area void (89 Å^2) followed by the heterochiral ***rac*-2ClO₄** (85 Å^2), and the areas of the voids in the homochiral complexes are much smaller (67−71 Å^2). As discussed, the heterochiral complexes have a more flattened and spread out skeletal structure, and the sheets are stacked with a shift. All these features contribute to providing a large channel and can accommodate larger anions and reduce the steric congestion between them.

Table 4 also lists the skeletal densities of the complexes, which were calculated by removing the counteranions and water molecules from the crystals, while the crystal structures were retained. The data obviously show that the homochiral complexes have higher densities; i.e., the 2D sheets are closely packed. In other words, a complex with small counteranions assumes a homochiral crystal structure with high density, because the anions can be accommodated in small channels, while a complex with large counteranions prefers a heterochiral channel structure to reduce the steric congestion.

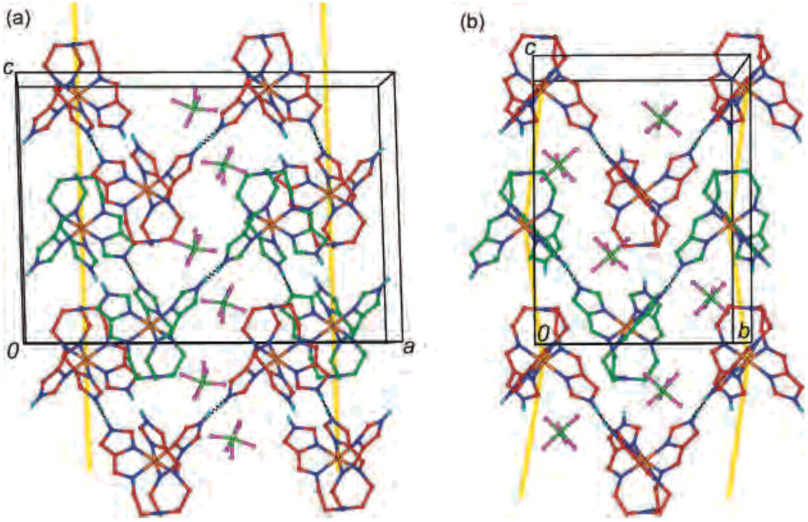

Figure 13. Crystal structure of $[Co(H_{1.5}L)](PF_6)_{1.5}\cdot 3.5H_2O$ (**2PF₆**) as viewed down the following: (a) the *ac*-plane; (b) the *bc*-plane. On the spreading out of the structure along the *a*-axis, a larger space is formed to accommodate $P(2)F_6^-$ ions. By a stacking of the sheets with a shift in the *b*-axis direction, as shown by the yellow zigzag lines, a large space is formed to accommodate the $P(1)F_6^-$ ions.

Table 4. Size of the Void and the Skeletal Density (a) of the Homochiral Crystals $[Co(H_{1.5}L)]Cl_{1.5}\cdot 4H_2O$ (**2Cl**), $[Co(H_{1.5}L)]Br_{1.5}\cdot 4H_2O$ (**2Br**), $[Co(H_{1.5}L)]I_{1.5}\cdot 2H_2O$ (**2I**), $[Co(H_{1.5}L)](BF_4)_{1.5}\cdot 2.5H_2O$ (**2BF₄**), and $[Co(H_{1.5}L)](ClO_4)_{1.5}\cdot H_2O$ (**2ClO₄**) and (b) of the Heterochiral Crystals *rac*-$[Co(H_{1.5}L)](ClO_4)_{1.5}\cdot 4H_2O$ (***rac*-2ClO₄**) and $[Co(H_{1.5}L)](PF_6)_{1.5}\cdot 3.5H_2O$ (**2PF₆**)

(a) homochiral cryst				(b) heterochiral cryst			
compd	av length of the sides of a triangle (Å)	area of a triangle[a] (Å²)	skeletal density[b] (g cm⁻³)	compd	av length of the sides of a triangle (Å)	area of a triangle[a] (Å²)	skeletal density[b] (g cm⁻³)
2Cl	12.62	69	1.195	***rac*-2ClO₄**	13.98	85	1.022
2Br	12.74	70	1.181	**2PF₆**	14.35	89	0.963
2I	12.44	67	1.165				
2BF4	12.71	70	1.203				
Λ-2ClO₄	12.76	71	1.195				

[a] Defined as the triangle formed by connecting the imidazole H(1) atoms (see Figures 4−8). [b] Calculated by removing the counteranions and water molecules from the crystals while the crystal structures were retained.

Concluding Remarks

We have shown that the hemideprotonated complexes studied (**2**) involve two component species, $[Co(H_3L)]^{3+}$ and [Co(L)], and components with the same absolute configuration are linked by imidazole−imidazolate hydrogen bonds to form a homochiral 2D puckered sheet structure. The sheet is composed of a hexanuclear unit with a trigonal void. There are two ways of stacking the sheets: one is homochiral stacking, where sheets with the same chirality are stacked to give a homochiral crystal (conglomerate); the other is heterochiral stacking, where a homochiral sheet consisting of Δ enantiomers and an adjacent sheet consisting of Λ enantiomers are stacked alternately to give a heterochiral crystal (a racemic crystal). There are two conflicting factors governing the crystal structure: the skeletal density; the size of the channels. Two-dimensional sheets are more closely packed in a homochiral crystal than in a heterochiral crystal, as evidenced by the high skeletal density (calculated by removing the counteranions and water molecules from the crystal). The homochiral crystals have smaller voids, and their skeletal structure is so rigid that steric congestion between the anions occurs as the anion size increases. Smaller anions, such as halide ions, can be accommodated in the *ab*-plane in a void. On the other hand, in the case of **2BF₄** and **Λ-2ClO₄**, 1/3 of the anions reside along the crystallographic C_3 axis to reduce the steric interaction between the anions. The heterochiral crystals have a flexible, zigzag channel structure, and the channel size can increase to accommodate larger anions. Thus, complex **2** with large anions (i.e., ClO_4^- and PF_6^-) forms a heterochiral crystal.

Experimental Section

Caution! *Perchlorate salts of metal complexes are potentially explosive. Only small quantities of material should be prepared, and the samples should be handled with care.*

Materials. All reagents and solvents used in the syntheses were of reagent grade, and they were used without further purification. $[Co(H_3L)](PF_6)_3\cdot 2H_2O$, $[Co(H_3L)](ClO_4)_3\cdot H_2O$ (**1ClO₄**), Λ-$[Co(H_3L)](ClO_4)_3\cdot 1.5H_2O$ (**Λ-1ClO₄**), $[Co(H_{1.5}L)]Cl_{1.5}\cdot 4H_2O$ (**2Cl**), and *rac*-$[Co(H_{1.5}L)](ClO_4)_{1.5}\cdot 4H_2O$ (***rac*-2ClO₄**) were prepared according to the literature procedure.[6,12]

$[Co(H_{1.5}L)]Br_{1.5}\cdot 3H_2O$ (2Br). An aqueous solution of $[Co(H_3L)](ClO_4)_3\cdot H_2O$ (0.38 g, 0.5 mmol) was stirred with an anion exchanger, Dowex 1 × 8 in the Cl^- form, and then the suspension was poured into a column (1.0 cm i.d. × 15 cm) of the same exchanger to ensure conversion to the chloride. The column was then washed with water. The effluent containing $[Co(H_3L)]Cl_3$ (0.5 mmol) was mixed with an aqueous solution of 1.0 M NaOH (0.75 mL, 0.75 mmol) and NaBr (0.515 g, 5.0 mmol). The mixture was concentrated using a rotary evaporator to give a reddish orange precipitate. Yield: 0.23 g (75%). Anal. Found: C, 35.40; H, 4.56; N, 22.88. Calcd for $[Co(H_{1.5}L)]Br_{1.5}\cdot 3H_2O = C_{18}H_{28.5}Br_{1.5}CoN_{10}O_3$: C, 35.34; H, 4.70; N, 22.90. IR (KBr disk): $\nu_{C=N}$

(imine) 1609, 1592 cm^{-1}. Crystals suitable for X-ray structural analysis were obtained from the filtrate after placing it in a refrigerator.

$[Co(H_{1.5}L)]I_{1.5}\cdot 2H_2O$ (2I). 1ClO$_4$ was converted into the chloride, $[Co(H_3L)]Cl_3$, using Dowex 1 × 8 (Cl^- form) in the same manner as for **2Br**. To an aqueous solution of $[Co(H_3L)]Cl_3$ (0.5 mmol) were added 1.0 M NaOH (0.70 mL, 0.7 mmol) and NaI (0.515 g, 5.0 mmol) in methanol to give red crystals. The product was a mixture of **2I** and **3I**, and these were separated on the basis of the difference in their densities. We used a solution ($CHBr_3$−toluene) with a density of 1.70 g mL^{-1}. **2I** sank, while **3I** floated. IR data for **2I** (KBr disk): $\nu_{C=N}$ (imine) 1600(sh), 1594 cm^{-1}.

$[Co(H_{0.5}L)]I_{0.5}\cdot 4H_2O$ (3I). This complex was prepared using the same procedure as for **2Br**, except that NaI was used instead of NaBr. Anal. Found: C, 37.83; H, 4.88; N, 24.17. Calcd for $[Co(H_{1.5}L)]I_{1.5}\cdot 4H_2O = C_{18}H_{29.5}CoI_{0.5}N_{10}O_4$: C, 37.77; H, 5.19; N, 24.47. IR (KBr disk): $\nu_{C=N}$ (imine) 1604, 1594 cm^{-1}.

$[Co(H_{1.5}L)](BF_4)_{1.5}\cdot 2.5H_2O$ (2BF$_4$). This complex was prepared using the same procedure as for **2Br**, except that $NaBF_4$ was used instead of NaBr. Yield: 42%. Anal. Found: C, 34.79; H, 3.74; N, 22.36. Calcd for $[Co(H_{1.5}L)](BF_4)_{1.5}\cdot 3H_2O = C_{18}H_{28.5}B_{1.5}CoN_{10}O_3$: C, 34.75; H, 4.62; N, 22.51. IR (KBr disk): $\nu_{C=N}$ (imine) 1600(sh), 15924 cm^{-1}; ν_{B-F} (BF_4^-) 1115, 1084, 1054, 1036 cm^{-1}.

$[Co(H_{1.5}L)](PF_6)_{1.5}\cdot 3.5H_2O$ (2PF$_6$). A 1.0 M NaOH (0.30 mL, 0.3 mmol) solution was added to a solution of $[Co(H_3L)](PF_6)_3\cdot 2H_2O$ (0.18 g, 0.2 mmol) in water−methanol. The mixture was filtered, and the filtrate was placed in a refrigerator to give orange-red crystals. Yield: 0.070 g (49%). Anal. Found: C, 30.13; H, 3.89; N, 19.39. Calcd for $[Co(H_{1.5}L)](PF_6)_{1.5}\cdot 3.5H_2O = C_{18}H_{29.5}CoF_{18}N_{10}O_{3.5}P_3$: C, 30.09; H, 4.14; N, 19.50. IR (KBr disk): $\nu_{C=N}$ (imine) 1628, 1602 cm^{-1}; ν_{B-F} (PF_6^-) 843 cm^{-1}.

Λ-$[Co(H_2L)][Sb_2((R,R)\text{-tart})_2]\cdot 4H_2O$. An aqueous solution of $[Co(H_3L)](ClO_4)_3\cdot H_2O$ (3.68 g, 5.0 mmol) was stirred with an anion exchanger, Dowex 1 × 8 in the Cl^- form, and then the whole suspension was poured into a column (1.0 cm i.d. × 15 cm) of the same exchanger to ensure conversion into the chloride. The column was washed with water. The effluent containing $[Co(H_3L)]Cl_3$ (5.0 mmol) was mixed with a suspension of $Ag_2[Sb_2((R,R)\text{-tart})_2]$ (3.76 g, 5.0 mmol; (*R*,*R*)-tart = (2*R*,3*R*)-tartrate(4−) ion) and $NaHCO_3$ (0.42 g, 5.0 mmol) in water. The mixture was stirred in the dark for 1 h and then filtered with Celite to remove AgCl. The filtrate was evaporated with a rotary evaporator to give a reddish orange precipitate. It was recrystallized from water. Yield: 1.79 g (35%). Anal. Found: C, 29.61; H, 3.23; N, 13.20. Calcd for $[Co(H_2L)][Sb_2((R,R)\text{-tart})_2]\cdot 4H_2O = C_{26}H_{35}CoN_{10}O_{16}Sb_2$: C, 29.85; H, 3.37; N, 13.39.

Λ-$[Co(H_3L)](ClO_4)_3\cdot 1.5H_2O$. The diastereomer Λ-$[Co(H_2L)][Sb_2((R,R)\text{-tart})_2]\cdot 4H_2O$ (**2**, 1.05 g, 1.0 mmol) was converted into the chloride by the use of Dowex 1 × 8 (Cl^- form) in the manner described for conversion of $[Co(H_3L)](ClO_4)_3\cdot H_2O$ into the chloride salt. An aqueous solution of Λ-$[Co(H_3L)]Cl_3$ (3.0 mmol) was mixed with $AgClO_4$ (0.622 g, 3.0 mmol), and the mixture was stirred for 1 h. AgCl was removed by filtration, and the filtrate was evaporated to give dark red crystals. Yield: 0.71 g (92%). Anal. Found: C, 28.14; H, 3.40; N, 18.0%. Calcd for $[Co(H_3L)](ClO_4)_3\cdot 1.5H_2O = C_{18}H_{27}Cl_3CoN_{10}O_{13.5}$: C, 28.27; H, 3.56; N, 18.32. IR (KBr disk): $\nu_{C=N}$ (imine) 1626; ν_{Cl-O} (ClO_4^-) 1142, 1117, 1088 cm^{-1}.

Λ-$[Co(H_{1.5}L)](ClO_4)_{1.5}\cdot H_2O$ (Λ-2ClO$_4$). Λ-$[Co(H_3L)](ClO_4)_3\cdot 1.5H_2O$ (0.382 g, 0.5 mmol) was converted into the chloride, Λ-$[Co(H_3L)]Cl_3$, using Dowex 1 × 8 (Cl^- form) in the same manner as for **2Br**. To an aqueous solution of Λ-$[Co(H_3L)]Cl_3$ (0.5 mmol) were added 1.0 M NaOH (0.75 mL, 0.75 mmol) and $NaClO_4$ (0.183 g, 1.5 mmol) in methanol to give red crystals. Yield: 0.268 g (89%). Anal. Found: C, 35.77; H, 4.26; N, 22.84. Calcd for $[Co(H_{1.5}L)](ClO_4)_{1.5}\cdot H_2O = C_{18}H_{24.5}Cl_{1.5}CoN_{10}O_7$: C, 35.73; H, 4.08; N, 23.15. IR (KBr disk): ν_{C}=**N** (imine) 1608, 1592 cm^{-1}; ν_{B}-F (ClO_4^-) 1144, 1117, 1087 cm^{-1}. UV−vis (MeOH): 480 (224), 320 nm (5000 M^{-1} cm^{-1}). CD (MeOH): 486 (−10.1), 347 nm (+27.3 M^{-1} cm^{-1}).

Physical Measurements. The UV−vis spectra were recorded using a JASCO Ubest-550 spectrophotometer. The infrared spectra were measured using a JASCO FT/IR-550 spectrophotometer. The CD spectra were recorded using a JASCO J-720 spectropolarimeter.

X-ray Data Collection, Reduction, and Structure Determination. The X-ray data were collected using a Rigaku R-AXIS RAPID II imaging plate area detector employing graphite-monochromated Mo Kα radiation ($\lambda = 0.710\ 73$ Å). The structures were solved using direct methods and refined using full-matrix least-squares procedures using the CrystalStructure crystallographic software package.[16] The absolute configuration was determined on the basis of the Flack parameters.[14]

Acknowledgment. This work was supported in part by Grants-in-Aid for Scientific Research (Nos. 16205010, 16750050, and 17350028) from the Ministry of Education, Science, Sports, and Culture of Japan and by the Iketani Science and Technology Foundation.

Supporting Information Available: CD spectra of **2Br**, **2I**, and **2BF$_4$** crystals and X-ray crystallographic files in CIF format for **2Br**, **2I**, **2BF$_4$**, **Λ-2ClO$_4$**, **2PF$_6$**, and **3I**. This material is available free of charge via the Internet at http://pubs.acs.org.

IC070286+

---

(16) *CrystalStructure 3.8; Crystal Structure Analysis Package*; Rigaku and Rigaku/MSC: The Woodlands, TX, 2001−2006.